Biosensors and Bioelectronics 25 (2010) 1509–1515

Contents lists available at ScienceDirect

Biosensors and Bioelectronics

journal homepage: www.elsevier.com/locate/bios

A portable microfluidic flow cytometer based on simultaneous detection of impedance and fluorescence

Segyeong Joo[a,1], Kee Hyun Kim[b,1], Hee Chan Kim[c,**], Taek Dong Chung[d,*]

[a] Department of Biomedical Engineering, Asan Medical Center, University of Ulsan College of Medicine, Seoul 138-736, Republic of Korea
[b] Interdisciplinary Program, Bioengineering Major, Graduate School, Seoul National University, Seoul 152-742, Republic of Korea
[c] Institute of Medical & Biological Engineering, Medical Research Center and Department of Biomedical Engineering, College of Medicine, Seoul National University, Seoul 110-799, Republic of Korea
[d] Department of Chemistry, Seoul National University, Seoul 151-747, Republic of Korea

ARTICLE INFO

Article history:
Received 31 August 2009
Received in revised form 9 November 2009
Accepted 11 November 2009
Available online 17 November 2009

Keywords:
Microfluidic flow cytometer
Particle-based assays
Cell analysis
Polymeric gel electrode
Impedance detection
Fluorescence detection

ABSTRACT

A portable microfluidic flow cytometer with dual detection ability of impedance and fluorescence was developed for cell analysis and particle-based assays. In the proposed system, fluorescence from microparticles and cells is measured through excitation by a light emitting diode (LED) and detection by a solid-stated photomultiplier (SSPM). Simultaneous impedometric detection provides information on the existence and size of microparticles and cells through polyelectrolyte gel electrodes (PGEs) operated by custom designed circuits for signal detection, amplification, and conversion. Fluorescence and impedance signals were sampled at 1 kHz with 12 bit resolution. The resulting microfluidic cytometer is $15 \times 10 \times 10\,cm^3$ in width, depth, and height, with a weight of about 800 g. Such a miniaturized and battery powered system yielded a portable microfluidic cytometer with high performance. Various microbeads and human embryonic kidney 293 (HEK-293) cells were employed to evaluate the system. Impedance and fluorescence signals from each bead or cell made classification of micro particles or cells easy and fast.

1. Introduction

Flow cytometry is a powerful and widely used tool in biological and clinical research due to its multifunctional capabilities of counting, characterizing, and sorting. Since the 1980s, flow cytometers have been used increasingly for a number of biological applications, as well as medical diagnostics, including bead-based immunoassays (Vignali, 2000). Fluorescence activated cell sorter (FACS) and Coulter counter are representative instruments that show the advancement and proliferation of flow cytometry. On the other hand, establishment of the micro total analysis system (μTAS) in 1990 (Manz et al., 1990) fueled research on living cells and bead-based assays that exploit microfluidics, so called lab-on-a chip (LOC) techniques (Dittrich and Manz, 2006; Myers and Lee, 2008; Wang et al., 2009; Weibel and Whitesides, 2006; West et al., 2008; Whitesides, 2006). Flow cytometry is an important research target because microfluidic chip-based flow cytometers require little sample usage, fast and accurate analysis, and precise control of fluids containing particles or cells (Chung and Kim, 2007; Huh et al., 2005). The tremendous potential of microfluidic flow cytometers have been well proven, not only for measurement of various physiochemical cell characteristics, but also for particle-based assays, such as immunoassays (Lim and Zhang, 2007) and nucleic acid hybridization (Brenner et al., 2000).

Typical flow cytometry comprises transporting and counting or examining of particles or cells suspended in a fluid stream. FACS utilizes optical detection and Coulter counter employs an electrical detection mechanism (Durack and Robinson, 2000). In general, optical detection is powerful for characterizing and thus screening particles or cells. For that reason, most chip-based flow cytometers employ an optical detection strategy in which fluorescence measurements in various manner are representative (Chen and Wang, 2009; Fu et al., 2008; Kang et al., 2008; Mao et al., 2009; Wang et al., 2008; Yang et al., 2008). However, conventional flow cytometers, such as FACS, need a number of components, including a high-power light source for excitation of fluorescent tags, a photon detector, and other optical components, including lens, filter, mirror, and so on. The sophisticated integration and alignment of these parts normally make the whole system bulky and expensive (Ateya et al., 2008; Godin et al., 2008). Compared with optical methods, electrical detection is relatively simple and easy to recognize and to count microparticles or cells. Nevertheless, it does not

* Corresponding author. Tel.: +82 2 880 4362; fax: +82 2 887 4354.
** Corresponding author. Tel.: +82 2 2072 2931; fax.: +82 2 745 7870.
E-mail addresses: hckim@snu.ac.kr (H.C. Kim), tdchung@snu.ac.kr (T.D. Chung).
[1] These authors contributed equally to this work.

0956-5663/$ – see front matter © 2009 Elsevier B.V. All rights reserved.
doi:10.1016/j.bios.2009.11.011

provide as much information as optical detection, especially when the testing sample is a mixture of several different particles or cells.

In these regards, simultaneous detection of both optical and electrical signals from a particle or cell would undoubtedly offer much more informative systems. Recently, a few examples of such a system were reported (Holmes et al., 2007; Wu et al., 2008). Holmes et al. (2007) placed a pair of platinum electrodes on upper and lower surfaces of a fluidic channel to measure impedance between two electrodes. For fluorescence detection, a typical configuration of laser and photomultiplier was used. Wu et al. (2008) demonstrated another system that utilized a resistive pulse sensor for particle counting and an avalanche photodiode for laser-excited fluorescence detection. However, both systems were still bulky and expensive, as they rely on laser excitation and commercially available data acquisition cards for signal acquisition. Achievement of a truly portable, informative, and practical flow cytometer essentially requires the realization of simultaneous detection of fluorescence and impedance along with low-cost, minimal power consumption, and miniaturization, without the loss of sensitivity and reliability.

This paper proposes a miniaturized flow cytometer that detects the microparticles or cells through fluorescence, as well as impedance by integration of specially designed optical units and polyelectrolyte gel electrodes (PGEs). The size, cost, and power consumption of the system were substantially reduced by employment of a high sensitive solid-state photomultiplier (SSPM) as a fluorescence detector, and a light emitting diode (LED) as an excitation source, instead of laser or mercury lamp. Although a few previous reports have suggested LED excitation for fluorescence detection in a microfluidic system (Hurth et al., 2008; Liu et al., 2007; Novak et al., 2007; Ren et al., 2009; Yang et al., 2009), they were limited to fluorescence detection setup. To the best of our knowledge, no example of an entirely miniaturized system or combination with simultaneous impedometric detection has been published. As an alternative to conventional vacuum photomultiplier tubes (PMTs), the SSPM or silicon photomultiplier is an emerging tool due to its high sensitivity, even allowing single photon detection (Buzhan et al., 2003; Finocchiaro et al., 2009). Unlike PMTs, the SSPM is rarely affected by ambient magnetic field. On the other hand, dc-based impedometric detection is considered most desirable for electrical detection because cell membranes behave like capacitors in an aqueous electrical circuit, and thereby impedance changes due to the presence of cells tend to be larger at a lower frequency. In addition, dc impedance measurements need an even simpler instrument than conventional ac measurements (Park et al., 2009). Inspired by these facts, recent reports have suggested a new opportunity for dc-based impedance measurements. PGEs were employed to conduct impedometric detection of microparticles and cells (Chun et al., 2005) and a further improved version showed its ability to quantify human red blood cells (Kim et al., 2009). The unique dc measurement of impedance in these works benefited from the resistive contact between PGE and solution. Cells passing between PGEs along a microchannel interfere with the ionic current so as to produce resistance changes proportional to corresponding cell sizes. In the present work, a microfluidic flow cytometer with light weight, portable size, battery operability, and high sensitivity was constructed by combining LED/SSPM for optical detection and PGE-based impedance detection. The fully integrated system was evaluated with living cells as well as synthetic beads.

2. Experimental

2.1. System design

A schematic view of the proposed system is shown in Fig. 1. The system consists of a high-intensity blue LED with a dominant wavelength between 460 and 475 nm (OVLGB0C6B9, Optek Technology, USA) as an excitation source, an SSPM (0611B4MM, Photonique SA, Switzerland) for fluorescence detection, a dichroic mirror (CM1-BS1, Thorlabs Inc., USA) for selective reflecting photons emitted from the LED not to reach the sensing region of SSPM, a custom spatial filter, a film filter (Wratten Gelatin Filter No. 25, Kodak, USA) for blocking lights with a shorter wavelength than that of the emitted fluorescence, a microfluidic chip with fluidic channels, and integrated PGEs for impedance detection, and signal acquisition circuits for both fluorescence and impedance. The acquired impedance signals contain information on number and size distribution of particles or cells. At the same time, fluorescence signals allow characterization of particles or cells.

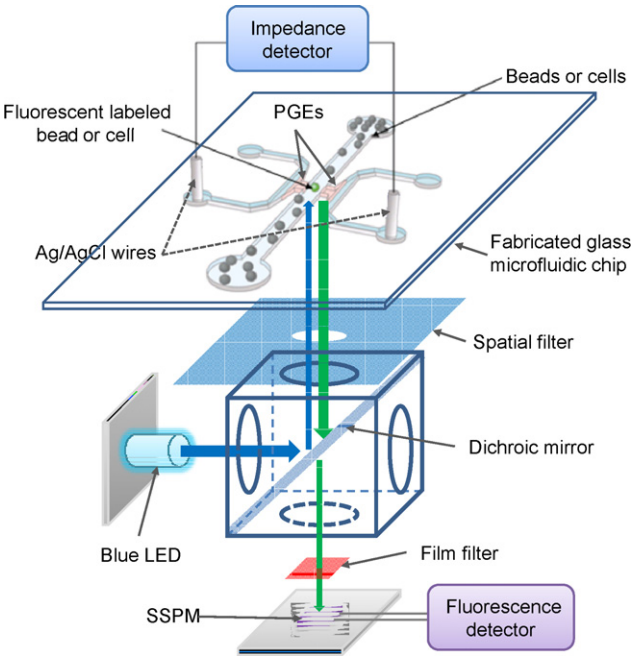

Fig. 1. Schematic diagram of the proposed microfluidic flow cytometer. Impedance between two PGEs integrated in a fabricated glass chip and fluorescence from a passing bead or cell are detected simultaneously with simple measurement setup. The figure is not to scale.

2.2. Chip fabrication

The glass chip with microfluidic channels and PGEs was prepared in a manner similar to one described in our previous reports (Chun et al., 2005; Kim et al., 2009). In brief, a slide glass (No.2947, Corning, USA) was cleaned with piranha solution (H_2O_2:H_2SO_4 = 1:3), then photoresist (PR) (AZ4620, Clariant, Switzerland) was spin-coated and patterned using conventional photolithographic techniques. The patterned PR played the role of a mask when the glass substrate was etched in a buffered oxide etchant solution (J.T. Baker, USA) for 35 min. The etched channel for sample flow and detection had internal dimensions of 70 μm in width and 30 μm in depth. After etching the fluidic patterns, holes were drilled to infuse solutions and the glass substrate was thermally bonded with another Corning 2947 glass. PGEs for impedance detection were constructed inside the bonded glass chip. To enhance adhesion of PGEs to the etched channels, 3-(trimethoxysilyl) propyl methacrylate (Sigma–Aldrich, USA) was coated on the channels. The mother solution for making PGEs contains diallyldimethylammonium chloride (DADMAC) (Sigma–Aldrich, USA) as a polymeric monomer, 2-hydroxy-40-(2-hydroxyethoxy)-2-methylpropiophenone (Sigma–Aldrich, USA) as photoinitiator, and *N*,*N*′-methylene-bisacrylamide (Sigma–Aldrich,

USA) as cross-linker. By exposing ultraviolet light onto the desired positions of the glass chip filled with the mother solution, photopolymerization of DADMAC was started, and thus PGEs were formed at the spot of interest. The size of the formed PGEs was 70 μm in width, 30 μm in depth, and 500 μm in length. For electrical connection of the PGEs with the measuring instrument, silver/silver chloride (Ag/AgCl) wires were immersed in the reservoirs that are separated from the main microchannel by PGEs. To minimize the resistance between PGEs and Ag/AgCl wires, each reservoir was filled with 1 M potassium chloride (KCl) solution (Sigma–Aldrich, USA). Figure S1 (see Supplementary Information) shows the fabricated microfluidic chip. Samples were delivered to the fluidic channel and flow was driven by hydraulic pressure.

2.3. Instrumentation for data acquisition

Fig. 2a shows the schematic diagram of the developed system for signal detection and data transmission. Impedance was monitored by continuous measurement of current between two PGEs facing each other, whilst a dc bias of 0.4 V was applied. The circuit for impedance detection imposes 0.4 V and converts measured current changes induced by the objects passing through the region between the two PGEs to corresponding voltage changes for amplification and display. Therefore, output voltage of the impedance detection circuit is proportional to the impedance between the two PGEs. To remove white noise, signals below 0.05 V after amplification were cut off to 0 V. The circuit for fluorescence detection based on an SSPM contains a high-voltage generator (TR-0.05P, Matsusada Precision Inc., Japan) to ensure bias voltage for Geiger mode operation of the SSPM and an amplifier for the current output from the SSPM. In order to simultaneously display both the impedance and fluorescence signals, background output voltage from the fluorescence detection circuit was set to 5 V in the absence of fluorescence. Current changes due to incident fluorescence photons were displayed in the form of proportional drops from 5 V. Signals output from circuits for impedance and fluorescence were converted by an embedded 12 bit analog-to-digital converter (ADC) (MCP3204, Microchip, USA) at the sampling rate of 1 kHz. For simpler calculation of acquired signals, dc 4.096 V signal (LT1790ACS6-4.096, Linear Technology, USA) was connected to the voltage reference pin of the ADC. As a consequence, amplified fluorescence signals over 4.096 V were read as 4.096 V, which helps to remove noise signals from the SSPM due to dark current or ambient light. Converted digital data was transferred to an 8-bit microcontroller unit (MCU) (ATmega8, Atmel, USA) via serial peripheral interface and processed within the MCU. The MCU communicated with a personal computer (PC) via universal serial bus (USB) interface to send the acquired data upon request from the user. Data transferred from

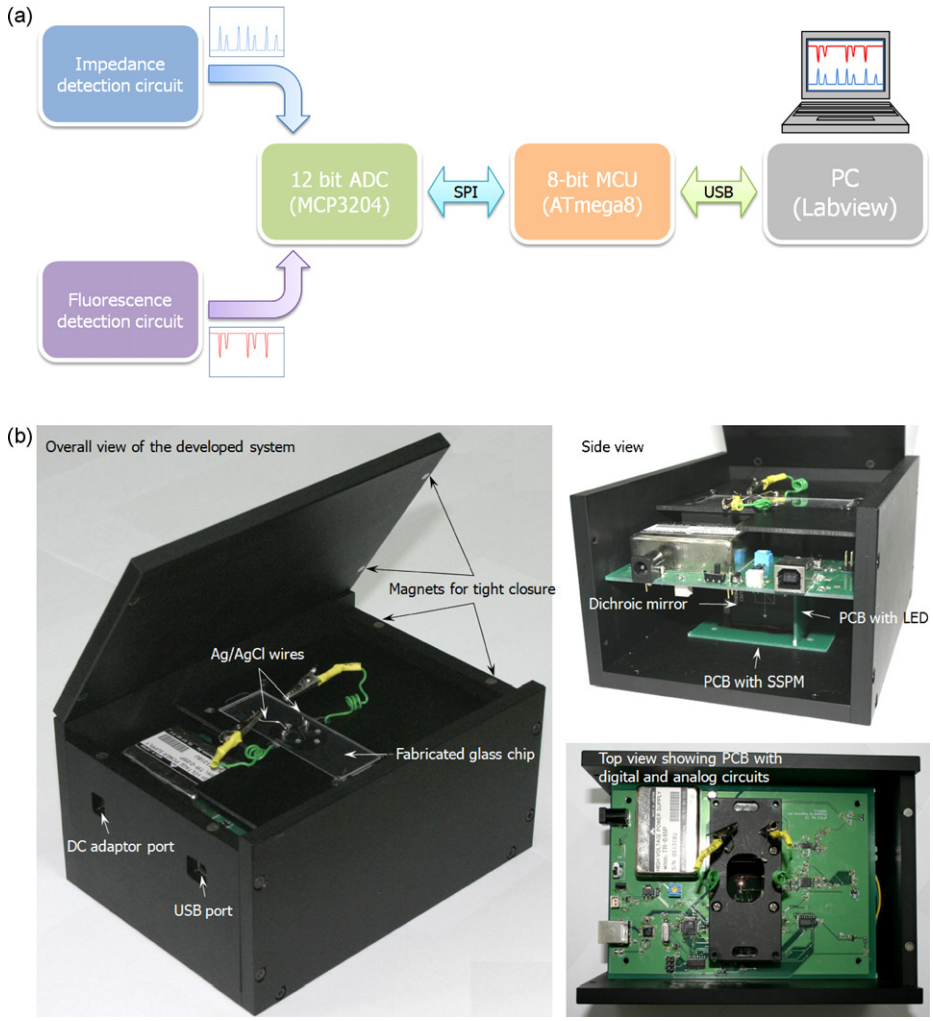

Fig. 2. (a) Schematic view of signal detection and transmission. Signals from impedance and fluorescence detection circuits are converted to digital by ADC and transmitted to MCU, which sends the acquired data to a PC via USB communication. (b) Pictures of the completed microfluidic flow cytometer. The overall view shows how the fabricated glass chip is placed on the system for measurement. The side view shows assembled dichroic mirror and PCBs with LED and SSPM. On the top view, PCB with digital and analog circuits for signal amplification and data processing is well shown.

the MCU was displayed and stored by custom software developed using Labview (National Instrument, USA). Fig. 2b shows the completed system. The entire system was encased in a black acryl box to be isolated from ambient light. The optical paths to LED and SSPM were aligned to meet each other at the center of the dichroic mirror. The fabricated chip was placed on the stage so that the microfluidic flow channel for particles or cells was situated vertically right above the center of the dichroic mirror. Circuits of amplifiers, ADC, and MCU were implemented on a custom printed circuit board (PCB). The developed cytometer system operated with either a single 9 V battery or a dc adapter. The size was 15 (width) × 10 (depth) × 10 (height) cm^3 and weight was about 800 g.

2.4. Sample preparation

Tests were carried out to check the function of the proposed system by employing various types of beads. Fluorescent beads having mean diameters of 5.78 (1% solid content, FC06F/8369, Bangs Laboratories, USA) and 10.35 μm (1% solid content, FC07F/5439, Bangs Laboratories, USA) and plain beads having mean diameters of 5.8 (10.4% solid content, PS06N/5665, Bangs Laboratories, USA) and 9.86 μm (10% solid content, PS06N/6955, Bangs Laboratories, USA) were purchased. Both types of fluorescent bead are excited at 480 nm and emit 520 nm. To prepare a mixture of plain and fluorescent bead solutions, 20 μL of fluorescent and 2 μL of plain bead solution were mixed and diluted in 1 mL of 1 M KCl solution prior to use. As a result, the numbers of fluorescent and plain beads in the mixture were similar.

To validate the proposed cytometer with live cells, human embryonic kidney 293 (HEK-293) cells were used. Green fluorescent protein (GFP) vector was transfected to cultured HEK-293 cells with Lipofectamine 2000 (Invitrogen, USA) in Opti-MEM I (Invitrogen, USA) medium for 18 h in a CO_2 incubator at 37 °C.

For both beads and cells, 1 mL of sample solution containing average 200 beads or cells were used. The prepared sample solution was flowed out in about 100 s with hydraulic pressure, which implies the flow rate was about 10 μL per second.

3. Results and discussion

3.1. Functional validation with fluorescent beads

First, the developed cytometer system was evaluated by one type of bead. Impedometric performance verification was performed by synchronization monitoring of microscopic view and impedance signal of the system after connecting the developed impedance detection circuit to a microscope. Fig. 3a shows acquired impedance and fluorescence signals when 10.35 μm fluorescent beads were used. For both impedance and fluorescence signals, every peak voltage due to the beads passing the region between a pair of PGEs exhibited very uniform levels near 0.9 V and 3.6 V for impedance and fluorescence, respectively. It should be noticed that impedance and fluorescence peaks were perfectly synchronized. One peak in fluorescence signal always comes with one peak of impedance signal. Neither false positive nor false negative case was monitored in the result. In the presence of only 9.86 μm plain beads, no peak was observed on the fluorescence side, while impedance signals responded to individual beads (see Figure S2 in Supplementary Information).

Tests with mixtures of fluorescent and plain beads were more informative. When a mixed sample of 9.86 μm plain beads and 10.35 μm fluorescent beads was used, impedance peaks appeared indiscriminately in response to all beads, whereas fluorescence peaks corresponded to only fluorescent beads that passed through (Fig. 3b). Finally, a sample containing four types of bead (mixture

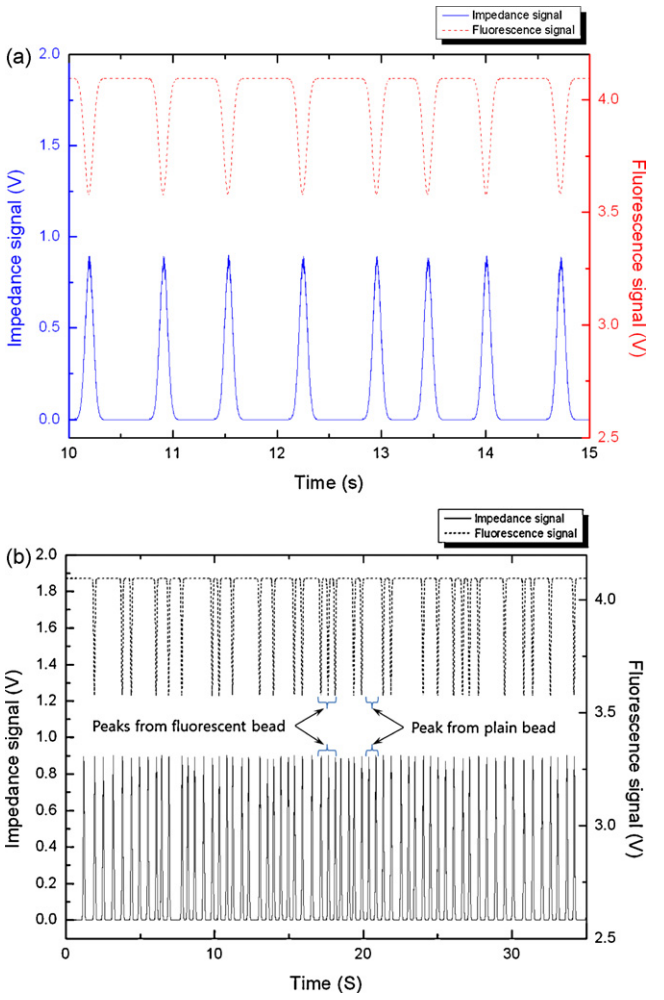

Fig. 3. (a) Acquired impedance and fluorescence signal of 10.35 μm fluorescent beads. Left and right vertical axes represent the magnitude of the impedance signal and the magnitude of the fluorescence signal. (b) Impedance and fluorescence signals of mixed sample of 9.86 μm plain beads and 10.35 μm fluorescent beads. Plain beads make peaks only on the impedance signal, whereas fluorescent beads make peaks on both impedance and fluorescence signals.

of 5.78 μm fluorescent beads, 10.35 μm fluorescent beads, 5.8 μm plain beads, and 9.86 μm plain beads) was tested. Fig. 4a shows impedance and fluorescence signals from the mixed sample. In accordance with the previous results, fluorescent beads produced both impedance and fluorescence peaks, while plain beads made only impedance peaks. Furthermore, the height of the impedance peaks reflects the size of the beads at the moment of passing between the PGEs. Fig. 4b shows the scatter plot of the beads on the basis of the peak height of the impedance and fluorescence signals. One can easily divide four groups as a function of the height of impedance and fluorescence peaks. Fluorescent beads having diameter of 10.35 μm are responsible for the 45 points at the lower-right corner, and their average impedance signal was 0.85 V with standard deviation (SD) of 4.1 mV and average fluorescence signal was 3.58 V with SD of 0.58 mV. Data from the 43 fluorescent beads of 5.78 μm in diameter are distributed at the middle-left side, and their corresponding average impedance signal was 0.21 V with SD of 1.1 mV and average fluorescence signal was 3.93 V with SD of 0.44 mV. Meanwhile, fluorescence signals from plain beads remain at 4.096 V, indicating no fluorescence. The 47 points at upper-right corner came from 9.86 μm plain beads, and their average impedance was 0.85 V with SD of 4.0 mV. Finally, 5.8 μm plain beads producing 50 impedance data that are found

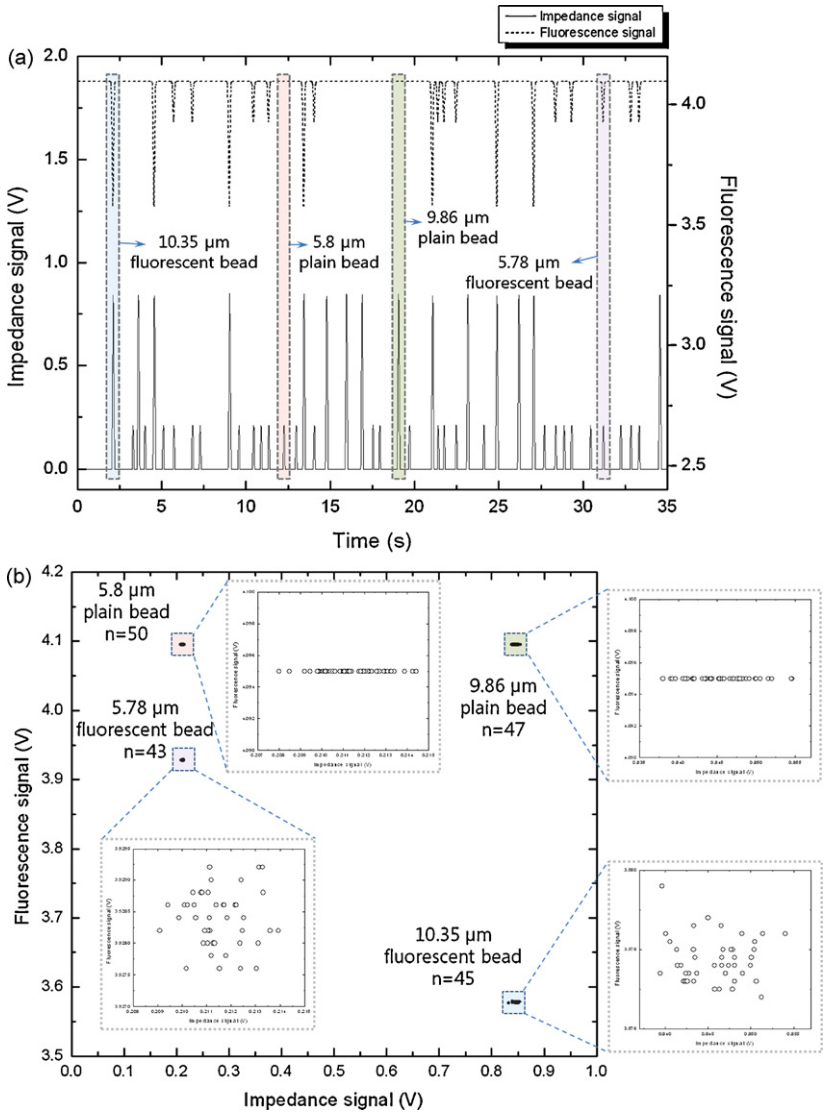

Fig. 4. (a) Impedance and fluorescence signals from a mixed sample of 5.78 μm fluorescent beads, 10.35 μm fluorescent beads, 5.8 μm plain beads, and 9.86 μm plain beads. (b) Scatter plot of every bead, with peak height value of impedance signal as horizontal axis and peak height value of fluorescence signal as vertical axis. Insets show an enlarged view of each group.

at upper-left corner showed average value of 0.21 V with SD of 1.4 mV.

Consequently, the test results unequivocally show that the developed device selectively recognizes the four different types of microparticles in terms of their size and fluorescence by aid of simultaneous measuring power of fluorescence as well as impedance. In addition, total numbers of each bead within the regions were 45, 43, 47, and 50 for 10.35 μm fluorescent beads, 5.78 μm fluorescent beads, 9.86 μm plain beads, and 5.8 μm plain beads, respectively. The numbers of each bead type are similar, which is consistent with the composition of beads in the sample solution.

3.2. Flow cytometric results with live cells

The developed cytometer was also tested with live cells to evaluate its function for biological applications. Figure S3 (see Supplementary Information) shows fluorescence and impedance signals from the developed system when untreated HEK-293 cells (Figure S3a) and GFP transfected HEK-293 cells (Figure S3b) were used as samples. Results are consistent with those expected from the plain and fluorescent beads. Impedance signals solely responded to the untreated HEK-293 cells, whereas GFP transfected HEK-293 cells gave rise to both impedance and fluorescence responses. Fig. 5a shows the response of the system to the mixture of untreated and GPF transfected HEK-293 cells with approximately same density. As shown in Fig. 5a, the mixed signals observed corresponded to untreated HEK-293 cells and GFP transfected HEK-293 cells. The scatter plot of the mixed sample (Fig. 5b) shows two types of cells clearly separable by the absence and presence of the fluorescence signals. Point counts for each type of cell were 55 and 51 for untreated HEK-293 cells and GFP transfected HEK-293 cells, respectively, confirming that the signals properly reflect the composition of untreated and GFP transfected cells.

The test with GFP transfected cells provides additional valuable information, that is, the efficiency of transfection. From the data as shown in Figure S3b, one can calculate the transfection ratio by dividing the number of fluorescence peaks by the number of impedance peaks. The average value was 99%, very close to the reference transfection ratio of 98.0%, which was measured by a commercial FACS machine (FACSCanto, Becton Dickinson and Company, USA) for the GFP transfected HEK-293 cells (n = 100,000)

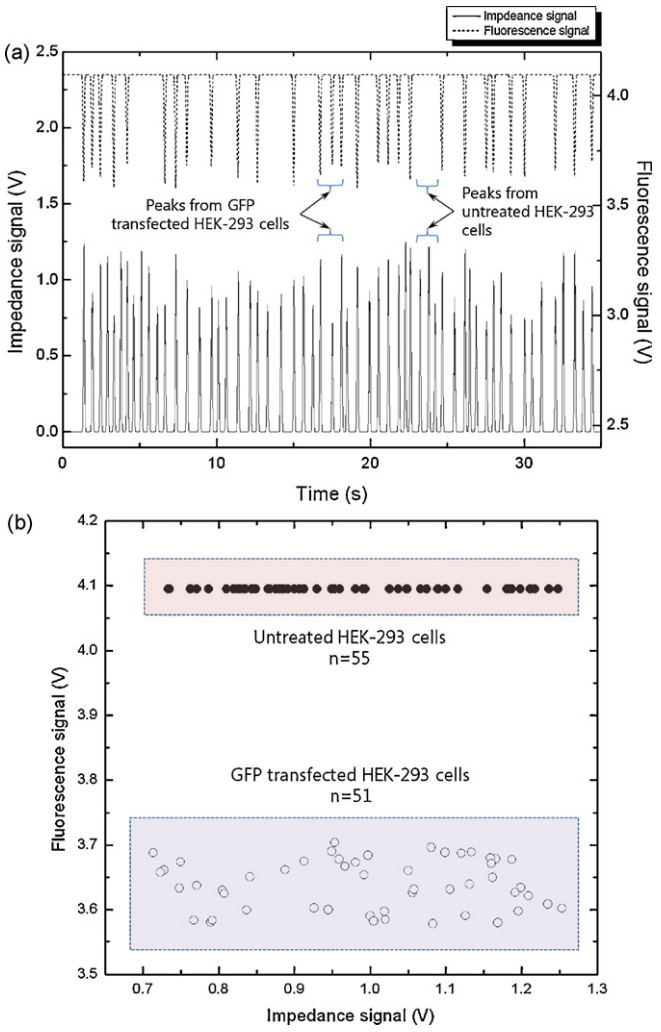

Fig. 5. (a) Impedance and fluorescence signals from a mixed sample of untreated HEK-293 cells and GFP transfected HEK-293 cells. (b) Scatter plot of every HEK-293 cell. Classification of two groups of untreated and GFP transfected HEK-293 cells can be done easily using the value of the fluorescence signal.

prepared in the same way. When compared with the scatter plot of Fig. 4b, impedance points of GFP transfected cells, as in Fig. 5b, are distributed more widely than the beads. This can be reasonably understood by considering the fact that commercial beads are uniformly spherical in shape, while living cells, particularly those flowing in a microchannel, are not supposed to be like the synthetic beads.

In the above experiments, the screening rate was about two samples per second due to the limitation of flow rate generated by hydraulic pumping method. However, this is comparable with the screening rate of about 100 particles per minute by the system developed by Holmes et al. (2007). The screening rate can be increased using a pump with higher output and a signal processing system with a higher sampling rate. The maximum screening rate of the developed system is far lower than that of commercial FACS devices. Since the microfluidic cytometer in this work is the first version to realize the fluorescence-impedance combination model on a chip, there is a tremendous potential to further increase its maximum screening rate. For instance, the system design could be substantially improved by adoption of a fast ADC, which is expected to raise the sampling rate up to several hundred kHz. Moreover, the fabrication procedure of the microfluidic network on a chip allows replication of the cytometric unit at negligible additional cost. Massively parallel cytometers integrated on a chip surely have a much higher screening rate.

4. Conclusion

We truly fabricated a new microfluidic flow cytometer that operates reliably and rapidly by simultaneous detection of impedance and fluorescence. The function of the developed cytometer is based on detection of impedance and fluorescence using on-chip integrated PGEs and semiconductor devices of LED and SSPM. The instrumentation for detection, amplification, and conversion of the two types of signal was implemented on a single custom-made PCB. The size and weight of the whole instrument were 15 (width) × 10 (depth) × 10 (height) cm^3 and 800 g, respectively, which is acceptable for a portable device. In addition, the system is battery operable. The functionality of the developed system as an entirely miniaturized cytometer was evaluated using synthetic microbeads and live HEK-293 cells, guaranteeing practical usage for various point-of-care testing (POCT). Impedance and fluorescence signals from each bead or cell were simultaneously monitored and utilized to classify micro particles or cells in a fast and easy way. This strongly suggests that the current system will evolve into a portable FACS by combining our previously developed pumping and sorting devices (Joo et al., 2007). Overall results indicate without ambiguity that the proposed cytometer in this work offers new opportunities in a wide range of applications, including bead-based immunoassay, drug screening at lower cost, high throughput stem cell collection, and many others.

Acknowledgements

This work was supported by Nano/Bio Science & Technology Program (M10536090001-05N3609-00110) of the Ministry of Education, Science and Technology (MEST), and by the MKE (Ministry of Knowledge Economy), Korea, under the ITRC (Information Technology Research Center) support program supervised by the NIPA (National IT Industry Promotion Agency) (NIPA 2009-(C1090-0902-0002)).

Appendix A. Supplementary data

Supplementary data associated with this article can be found, in the online version, at doi:10.1016/j.bios.2009.11.011.

References

Ateya, D.A., Erickson, J.S., Howell Jr., P.B., Hilliard, L.R., Golden, J.P., Ligler, F.S., 2008. Analytical and Bioanalytical Chemistry 391 (5), 1485–1498.
Brenner, S., Johnson, M., Bridgham, J., Golda, G., Lloyd, D.H., Johnson, D., Luo, S., McCurdy, S., Foy, M., Ewan, M., Roth, R., George, D., Eletr, S., Albrecht, G., Vermaas, E., Williams, S.R., Moon, K., Burcham, T., Pallas, M., DuBridge, R.B., Kirchner, J., Fearon, K., Mao, J.I., Corcoran, K., 2000. Nature Biotechnology 18 (6), 630–634.
Buzhan, P., Dolgoshein, B., Filatov, L., Ilyin, A., Kantzerov, V., Kaplin, V., Karakash, A., Kayumov, F., Klemin, S., Popova, E., Smirnov, S., 2003. Nuclear Instruments and Methods in Physics Research Section A: Accelerators, Spectrometers, Detectors and Associated Equipment 504 (1–3), 48–52.
Chen, H.T., Wang, Y.N., 2009. Microfluidics and Nanofluidics 6 (4), 529–537.
Chun, H., Chung, T.D., Kim, H.C., 2005. Analytical Chemistry 77 (8), 2490–2495.
Chung, T.D., Kim, H.C., 2007. Electrophoresis 28 (24), 4511–4520.
Dittrich, P.S., Manz, A., 2006. Nature Reviews Drug Discovery 5 (3), 210–218.
Durack, G., Robinson, J.P., 2000. Emerging tools for single-cell analysis. Wiley-Liss, New York.
Finocchiaro, P., Pappalardo, A., Cosentino, L., Belluso, M., Billotta, S., Bonanno, G., Di Mauro, S., 2009. IEEE Transactions on Nuclear Science 56 (3), 1033–1041.
Fu, L.M., Tsai, C.H., Lin, C.H., 2008. Electrophoresis 29 (9), 1874–1880.
Godin, J., Chen, C.H., Cho, S.H., Qiao, W., Tsai, F., Lo, Y.H., 2008. Journal of Biophotonics 1 (5), 355–376.
Holmes, D., She, J.K., Roach, P.L., Morgan, H., 2007. Lab on a Chip – Miniaturization for Chemistry and Biology 7 (8), 1048–1056.
Huh, D., Gu, W., Kamotani, Y., Grotberg, J.B., Takayama, S., 2005. Physiological Measurement 26 (3).

Hurth, C., Lenigk, R., Zenhausern, F., 2008. Applied Physics B: Lasers and Optics 93 (2–3), 693–699.
Joo, S., Chung, T.D., Kim, H.C., 2007. Sensors and Actuators, B: Chemical 123 (2), 1161–1168.
Kang, Y., Wu, X., Wang, Y.N., Li, D., 2008. Analytica Chimica Acta 626 (1), 97–103.
Kim, K.B., Chun, H., Chan, K.H., Chung, T.D., 2009. Electrophoresis 30, 1–6.
Lim, C.T., Zhang, Y., 2007. Biosensors and Bioelectronics 22 (7), 1197–1204.
Liu, C., Cui, D., Chen, X., 2007. Journal of Chromatography A 1170 (1–2), 101–106.
Manz, A., Graber, N., Widmer, H.M., 1990. Sensors and Actuators B: Chemical 1 (1–6), 244–248.
Mao, X., Lin, S.C.S., Dong, C., Huang, T.J., 2009. Lab on a Chip – Miniaturization for Chemistry and Biology 9 (11), 1583–1589.
Myers, F.B., Lee, L.P., 2008. Lab on a Chip – Miniaturization for Chemistry and Biology 8 (12), 2015–2031.
Novak, L., Neuzil, P., Pipper, J., Zhang, Y., Lee, S., 2007. Lab on a Chip – Miniaturization for Chemistry and Biology 7 (1), 27–29.
Park, S., Chung, T.D., Kim, H.C., 2009. Microfluidics and Nanofluidics 6 (3), 315–331.
Ren, K., Liang, Q., Mu, X., Luo, G., Wang, Y., 2009. Lab on a Chip – Miniaturization for Chemistry and Biology 9 (5), 733–736.
Vignali, D.A.A., 2000. Journal of Immunological Methods 243 (1–2), 243–255.
Wang, J., Bao, N., Paris, L.L., Geahlen, R.L., Lu, C., 2008. Analytical Chemistry 80 (24), 9840–9844.
Wang, J., Ren, L., Li, L., Liu, W., Zhou, J., Yu, W., Tong, D., Chen, S., 2009. Lab on a Chip – Miniaturization for Chemistry and Biology 9 (5), 644–652.
Weibel, D.B., Whitesides, G.M., 2006. Current Opinion in Chemical Biology 10 (6), 584–591.
West, J., Becker, M., Tombrink, S., Manz, A., 2008. Analytical Chemistry 80 (12), 4403–4419.
Whitesides, G.M., 2006. Nature 442 (7101), 368–373.
Wu, X., Chon, C.H., Wang, Y.N., Kang, Y., Li, D., 2008. Lab on a Chip – Miniaturization for Chemistry and Biology 8 (11), 1943–1949.
Yang, F.B., Pan, J.Z., Zhang, T., Fang, Q., 2009. Talanta 78 (3), 1155–1158.
Yang, S.Y., Lien, K.Y., Huang, K.J., Lei, H.Y., Lee, G.B., 2008. Biosensors and Bioelectronics 24 (4), 855–862.